Particle simulation of energetic particle driven Alfvén modes*

G. Vlad 1), S. Briguglio 1), C. Di Troia 1), G. Fogaccia 1), F. Zonca 1), K. Shinohara 2), M. Ishikawa 2), M. Takechi 2), W.W. Heidbrink 3), M.A. Van Zeeland 4), A. Bierwage 3), X. Wang 5)
1) Associazione EURATOM-ENEA, Frascati, (Rome) Italy
2) Japan Atomic Energy Agency, Naka, Ibaraki 311-0193, Japan
3) University of California, Irvine, California, USA
4) General Atomics, San Diego, California, USA
5) IFTS, Zhejiang University, Hangzhou, People's Republic of China
*This work was partially supported by the U.S. Department of Energy
e-mail contact of main author: vlad@frascati.enea.it

Abstract. The results of hybrid MHD-particle simulations of the Alfvén mode dynamics in a reversed-shear beam-heated DIII-D discharge are reported and compared with the experimental observations. Specific attention is devoted to the inclusion, in the numerical model, of nonlinear coupling between different toroidal mode numbers.

1. Introduction

The transport of fast ions produced by fusion reactions and/or auxiliary heating can be enhanced by their resonant interaction with the Alfvén modes. Theoretical [1, 2, 3] and numerical work [4, 5] has shown, in particular, that rapid transport of fast ions can take place because of fast growing Energetic Particle driven Modes (EPMs) [6]. EPMs have been proposed to generate "avalanches", that is convectively amplified mode structures nonlinearly evolving on the same time scale of the ballistic fast-ion transport and following the radially moving unstable front; evidence of this phenomenology has also been observed, in fact, in numerical simulations [1].

Plasma regimes in which enhanced fast ion transport occurs because of strongly driven EPMs should indeed be avoided in order to reach reactor relevant performance and prevent first wall damage. The investigation of the transition from regimes characterized by weakly driven modes (like, e.g., Toroidal Alfvén Eigenmodes, TAEs) to regimes dominated by strongly driven modes (like EPMs) and the determination of the related threshold are then of a crucial importance for burning plasma operations. Hybrid MHD-particle codes are able to address these issues, as they retain particle-wave interactions in a self-consistent, rather than perturbative, way.

The Hybrid MHD-Gyrokinetic code (HMGC [7]) has been used in the past [8] to predict both Alfvén mode and energetic particle dynamics for future burning plasma scenarios (e.g. for ITER). In order to assess these predictions, the code has to be validated with respect to the phenomena observed in present experiments, characterized by large fractions of fast ions. Such a validation has already been carried out for the case of negative neutral beam (NNB) heated JT60-U discharges. In these discharges, two types of bursting modes are observed by MHD spectroscopy [9]. The first one, called Abrupt Large-amplitude Event (ALE), is characterized by a time scale of the order of 100 μs, a relatively large fluctuating magnetic field at the first wall, wide frequency spectra in the range of the Alfvén frequency and a significant decrease of the fast ion density in the center of the discharge. The second mode is observed during the relative quiescent phase between two consecutive ALEs. It is characterized by a longer time scale (few milliseconds), narrower frequency spectra, lower fluctuating field level and modest energetic ion redistribution than the ALE case. A peculiar characteristic of this mode is its chirping up and down in frequency: it has then been dubbed fast Frequency Sweeping (FS)

mode. Simulations performed by HMGC show [10] that the ALE dynamics can be explained in terms of the nonlinear behaviour of a fast growing EPM. The simulation of the almost quiescent phase following the ALE event compares well with the fast FS phenomenology, as well, provided that modifications of the fast ion distribution function induced by the EPM saturation both in configuration (density profile) and velocity space are retained.

In the present paper, we want to further benchmark HMGC by applying it to the case of reversed-shear beam-heated DIII-D discharges. The plasma model adopted in HMGC consists of a thermal (core) plasma and an energetic-ion population. The former is described by reduced $O(\epsilon^3)$ MHD equations [11, 12] in the limit of zero pressure (ϵ being the inverse aspect ratio of the torus), including resistivity and viscosity terms; this model allows to investigate only equilibria with shifted circular magnetic surfaces. The fast ion population is described by the nonlinear gyrokinetic Vlasov equation [13, 14], expanded in the $k_\perp \rho_H \ll 1$ limit (with $k_\perp$ the component of the wave vector perpendicular to the magnetic field and ρ_H the energetic-ion Larmor radius), but fully retaining magnetic drift orbit widths and solved by particle-in-cell (PIC) techniques. The coupling between energetic ions and thermal plasma is obtained through the divergence of the energetic-ion pressure tensor, which enters the vorticity equation [15]. Numerical simulations of experimental conditions are performed after fitting the relevant machine and thermal-plasma quantities – the on-axis equilibrium magnetic field, major and minor radii (R_0 and a, respectively), the safety-factor q, the electron n_e and ion n_i plasma densities, the electron temperature T_e –, the fast ion distribution function and the ratio β_H between fast ion and magnetic pressures.

2. Numerical Simulation of a Reversed-Shear Beam-Heated DIII-D Discharge

A rich spectrum of oscillations in the Alfvénic frequency range has been observed in DIII-D tokamak discharges characterized by reversed-shear q-profile and heated by neutral beams [16]. During the phase of the discharge characterized by Alfvénic activity, the energetic particle density profile, calculated by a classical deposition model (TRANSP code [17]), appears to be much more peaked than that observed experimentally, as inferred, e.g., from the Fast Ion D_α (FIDA) diagnostic or from EFIT [18] equilibrium magnetic flux reconstructions that use MSE (Motional Stark effect), magnetic measurements, and thermal pressure data.

Here, we analyze shot #122117 at $t = 0.410$ s. The equilibrium configuration is characterized by $R_0 = 1.688\mathrm{m}$, $a = 0.609\mathrm{m}$, on-axis magnetic field $B_0 = 2\mathrm{T}$ and a reversed-q profile ($q_0 \approx 5$, $q_{min} \approx 4$, $q_a \approx 10.5$). The beam parameters are the following: average birth energy $E_0 = 0.077$ MeV (2/3 of the beams have birth energy of 0.075 MeV, and the residual 1/3 has 0.081 MeV), tangential radius $R_{tan} = 1.15\mathrm{m}$, parallel-to-perpendicular fast ion pressure ratio $p_{par}/p_{perp} \approx 1.44$, on-axis fast ion $\beta_{H0} \approx 0.8\%$, $m_H/m_i = 1$.

We first consider the results of single toroidal mode number simulations ($n = 2 - 4$, the dominant modes observed in the experiment), which fully retain energetic particle nonlinearities, while neglecting mode-mode coupling (the effects of this coupling will be addressed in the following Section). Initial fast ion distribution function is assumed to be an anisotropic slowing-down, with parameters fixed in such a way to reproduce beam features. Assuming the TRANSP simulation result as initial fast ion density profile, strongly unstable modes are observed, which cause a violent redistribution of the fast ions for all the simulated toroidal mode numbers. In FIG. *1.*, the fast ion profiles for the $n = 2$ simulation are shown: the

initialized TRANSP profile (black solid curve), the saturated profile (blue dashed curve). The saturated profile is strongly modified with respect to the initial one, in particular in its central value and width; it is clearly close to the fast ion profile obtained from equilibrium reconstruction, which is also reported for comparison (green dotted curve). Similar results are obtained for the $n = 3$ and $n = 4$ cases. In FIG. 2., the power spectra of the electrostatic potential during the linear growth (top) and the saturated phase (bottom) of the simulation are shown for the different toroidal mode numbers considered. Dominant modes are localized at the q_{min} radial position. Several very low frequency modes are also observed in the saturated phase, which can be identified as resistive MHD modes (resistivity

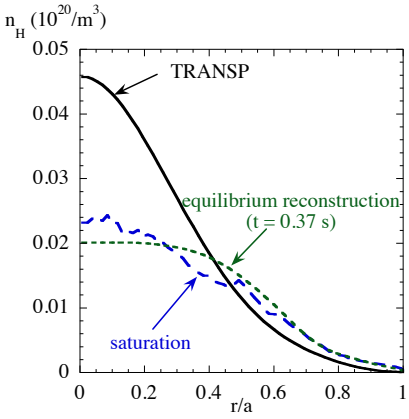

FIG. 1.: Fast ion density profiles as computed by TRANSP (black solid curve), by experimental reconstruction of equilibrium (green dotted curve) and as obtained by HMGC simulation after nonlinear saturation (blue dashed curve).

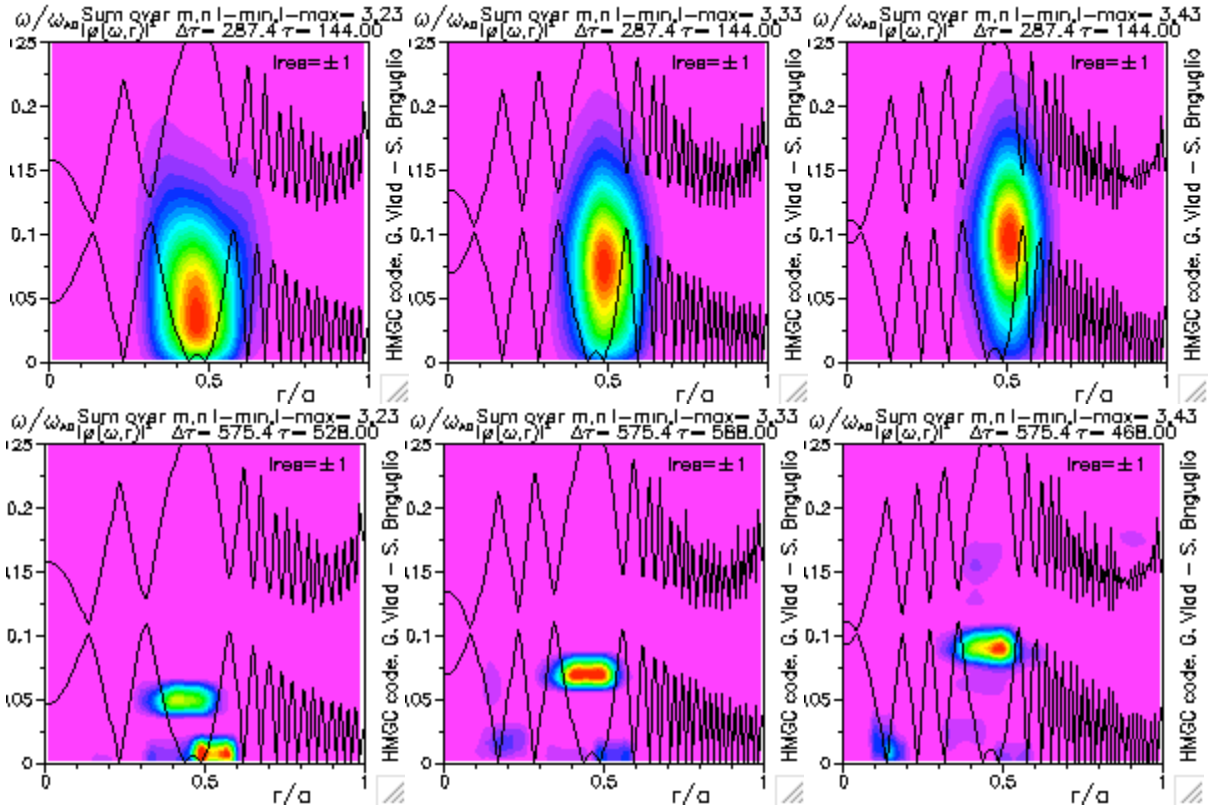

FIG. 2.: Power spectra of the scalar potential for $n = 2$ (left), $n = 3$ (center), and $n = 4$ (right). Ordinate is $\omega\tau_{A0}$, the Alfvén time in the center being $\tau_{A0} \approx 2.38194 \times 10^{-7}$ s. Fast ion initial density profile is from TRANSP. Top: linear phase, bottom: saturated phase.

is necessary for numerics; note that low-frequency activity due to geodesic curvature effects on shear Alfvén waves are not presently included in the HMGC code), along with weaker Alfvén modes localized inside the toroidal gap (at least, in the $n = 4$ case).

From this set of simulations, we can draw the following conclusions: (a) the equilibrium profile computed by TRANSP, which neglects energetic particle collective excitations, is strongly un-

stable once Alfvén wave dynamics is accounted for; (b) the collective mode dynamics causes a relevant flattening of the energetic particle density profile; (c) the saturated state is close to that reconstructed experimentally (by EFIT and/or FIDA); (d) the experimental profile could then be the consequence of a short time scale collective phenomenon.

Assuming that the experimental fast ion profile results from the effect of a short time scale collective phenomenon, we first compare qualitative and quantitative features of the experimentally observed frequency spectra of the modes with those by HMGC simulations. In this respect, the main qualitative feature is certainly represented by the sensitive dependence of the mode frequency on the minimum-q value, which is typical of so-called Reversed Shear Alfvén Eigenmodes (RSAEs) [19], also known as Alfvén Cascades (AC) [20]. Figure *3.* (top) shows

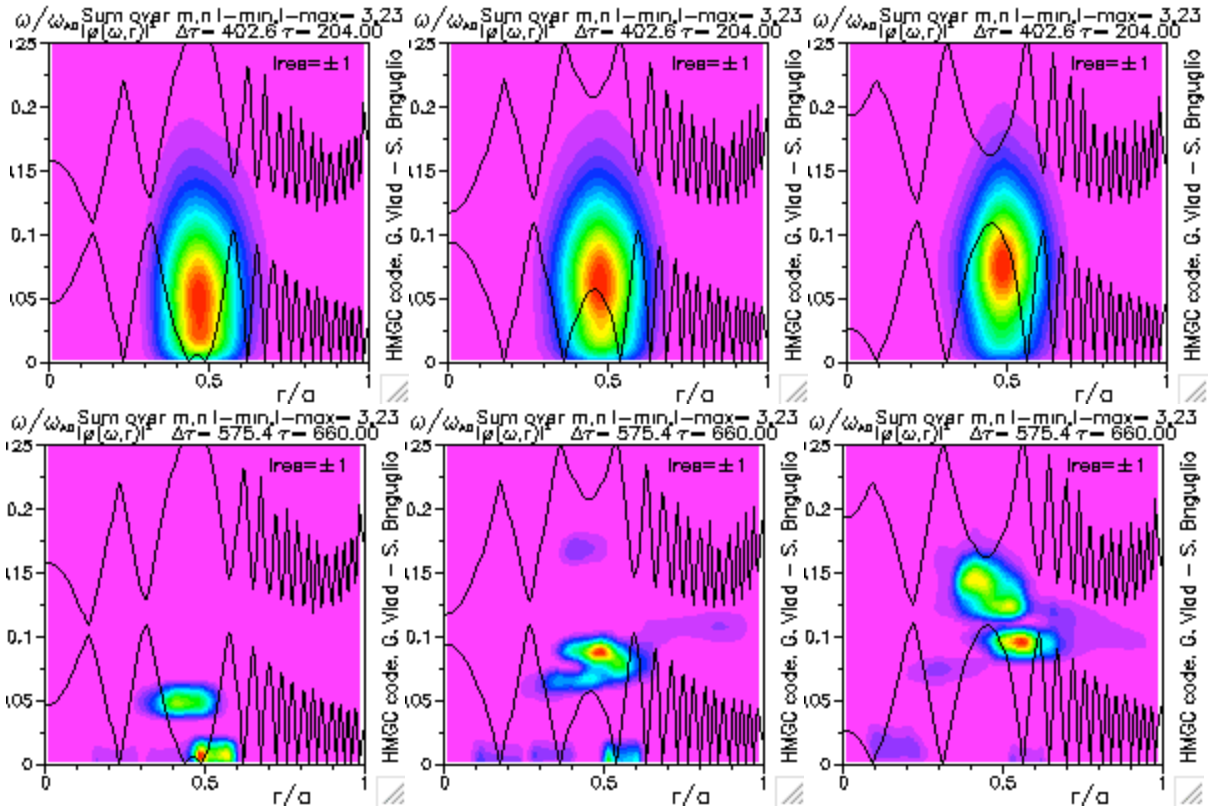

FIG. 3.: *Power spectra for* $n = 2$ *and* $q_{min} = 3.99$ *(nominal value, left),* $q_{min} = 3.89$ *(center),* $q_{min} = 3.79$ *(right) simulations initialized with TRANSP fast ion density profile. Top: linear phase. Bottom: saturated phase.*

the power spectra obtained for $n = 2$ for three different values of q_{min} during the linear mode growth. It is apparent that the frequency of the mode is weakly affected by the q_{min} variation and the corresponding modification of the Alfvén continuum. This is not surprising because the considered modes, in the linear phase, are strongly driven by energetic particles and, hence, their frequency is mainly determined by wave-particle resonance condition. After the large energetic particle redistribution (saturated phase), we expect that the weaker residual modes recover the experimentally observed dependence on q_{min} variations. This is confirmed by FIG. *3.* (bottom).

From a quantitative point of view, the comparison between simulation results and experimental frequencies [21] is less satisfactory. This is not surprising, taking into account the strong dependence of the saturated mode frequency on q_{min} and the uncertainties in the determination of such quantity: a little difference in the MSE-based evaluation of q would imply a large differ-

ence in the saturated mode frequency resulting from the simulation. Indeed, the best agreement for the considered case is shown in FIG. *4.*, which refers to $q_{min} \approx 3.89$ slightly smaller than the nominal value $q_{min} \approx 4$, though well within the experimental error bars. Another factor that may cause the simulated frequencies to be below those of experiment is the lack of compressibility effects in the HMGC model. Indeed finite thermal plasma pressure effects are most pronounced near the minimum of the RSAE frequency evolution (at $q_{min} = 4$) and in fact can dominate the mode frequency [22].

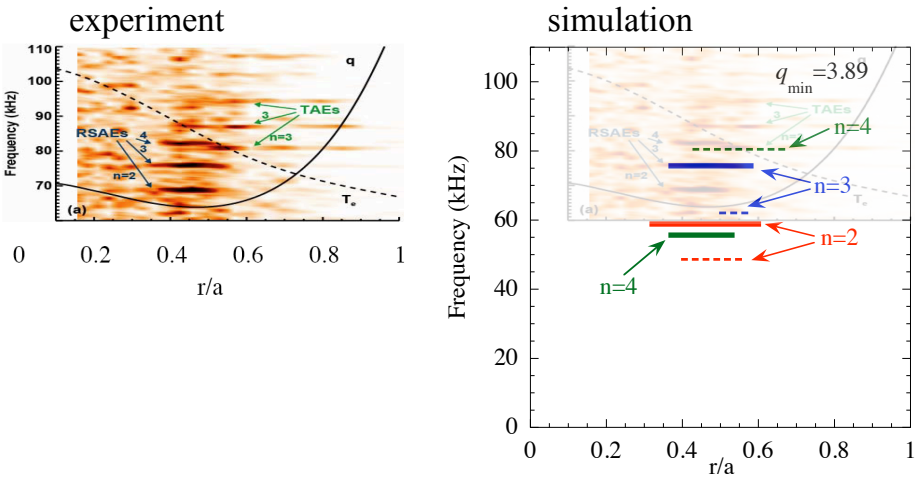

FIG. 4.: *Experimental frequency spectrum (left), and single-n simulation results (right) with slightly modified ($q_{min} = 3.89$) safety factor profile (two modes for each n are shown: the dominant ones – thick continuum lines – and the subdominant ones – thin dashed lines); the radial extension of the lines indicates the radial mode width.*

Another interesting quantitative comparison between simulations and experiments concerns the amplitudes of the perturbed magnetic field. The value obtained at $r/a \approx 0.45$, where the mode is localized, in the saturated phase of the $n = 2$ TRANSP-profile simulation considered in FIG. *2. left* (nominal q profile) is of order $\delta B_\theta/B_0 \approx 1.8 \times 10^{-3}$. This value is rather larger than the typical peak mode amplitudes inferred from MHD modeling, which are in the range $\delta B_\theta/B_0 \approx 5 \times 10^{-5} - 5 \times 10^{-4}$.

3. Fully nonlinear simulations

The results described in the previous Section refer to single-mode simulations neglecting mode-mode coupling. The reasonable agreement between the fast ion density profile found in numerical simulations after saturation and that measured experimentally can be considered as indication that fast growing modes (not directly observed in the experiments) and their nonlinear interaction with energetic particles ultimately determine fast ion profiles. In order to corroborate this hypothesis, however, we have to confirm that agreement persists once the simultaneous effect of all relevant toroidal modes is taken into account. Moreover, extending our numerical analysis to the lower growth-rate toroidal numbers ($n = 1$ and $n = 5$), contiguous to those considered first, we find that $n = 1$ modes yield a displacement comparable to that obtained, e.g., in the $n = 2$ case, while the $n = 5$ modes produce negligible fast ion displacement. This can be seen from the curves labelled with full circles and squares in FIG. *7.* (left, discussed below), which correspond to $n = 1$ and $n = 2$ single-mode simulations, respectively. In this Section, the preliminary results of a multi-mode $n = 0 - 5$ simulation (including mode-mode coupling) of the same discharge considered in the previous Section are presented. Some of nonlinear dynamics effects are still neglected; in particular, the evolution of the $m = 0, n = 0$

component of the fluctuating potentials is neglected, as well as of the $m = 1, n = 0$ component of the fast ion drive. The reason for the former approximation is that the MHD model itself is not suited to properly describe the evolution of the $m = 0, n = 0$ equilibrium component. The reason for the latter is to avoid spurious dynamics effects due to the fact that the initial fast ion distribution function is not expressed in terms of conserved quantities of particle motion.

Figure *5.* shows the energy content of the dominant poloidal component for each of the retained toroidal numbers versus time. We note that in a first purely-linear growth phase, modes with $n = 2$ and $n = 3$ exhibit the highest growth rates. As mode-mode coupling becomes important ($t \gtrsim 150\omega_{A0}^{-1}$), the interaction between $n = 2$ and $n = 3$ enhances the growth rate of $n = 5$ and, especially, $n = 1$ modes. The former modes eventually saturate, giving rise to fast ion displacement ($t \approx 190\omega_{A0}^{-1}$). The $n = 1$ mode, once the drive represented by mode-mode coupling is exhausted, is still driven by the residual fast ion density gradient closer to magnetic axis. Then, it further grows ($t \gtrsim 200\omega_{A0}^{-1}$) and eventually produces further ion density flattening, reaching saturation itself ($t \gtrsim 370\omega_{A0}^{-1}$). Figure *6.* presents the power spectra of the scalar potential during the linear growth phase (top) and after complete saturation (bottom) for the multi-mode simulation. Global (all n) spectra (left) are compared with the $n = 1$ (centre) and $n = 2$ (right) ones. As observed, the linear-growth phase is dominated by the $n = 2$ mode, while the $n = 1$ mode prevails in the saturated phase.

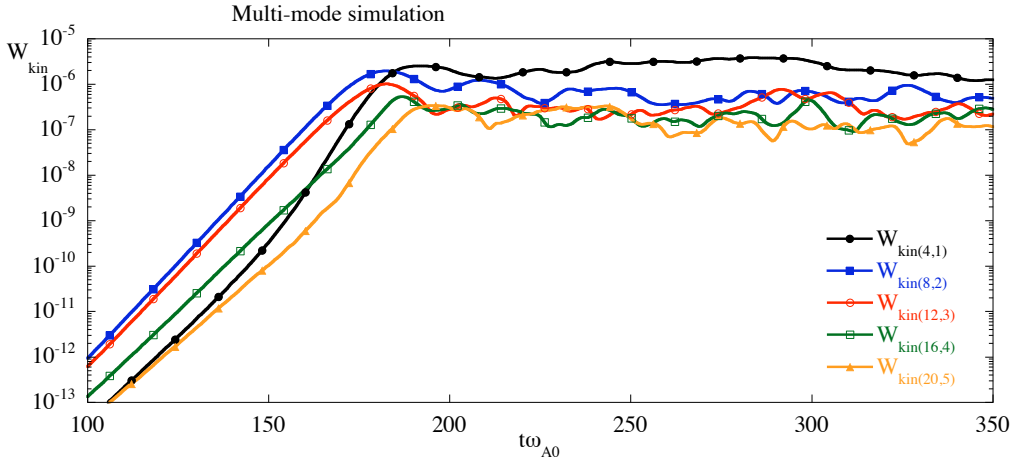

FIG. 5.: *Fully nonlinear multi-mode simulation: kinetic energy content of the dominant poloidal harmonics for different n values.*

The overall effect on the fast ion density profile is of the same order of that obtained in the single-mode simulations (see FIG. *7.* (left)). In the present case, both competition of different-n modes in extracting energy from resonant particles (as expected for EPMs), thereby flattening the fast ion profile, and the energy transfer from fast to slower growing modes by mode-mode coupling cause each toroidal mode to saturate at a lower level than that reached in the corresponding single-mode simulation. This is shown in FIG. *7.* (right), which compares the saturation levels obtained, in single-mode and multi-mode simulations, for the dominant poloidal harmonics of the poloidal electric field (responsible for fast ion convective displacement) corresponding to different n values. The observed reduction of the saturation levels goes in the direction of a better agreement between the simulation perturbed field levels and those inferred from the MHD modeling.

The results of multi-mode simulations, presented here, indicate that the low-frequency $n = 1$ mode is even more relevant, in the saturated phase, than the experimentally observed modes

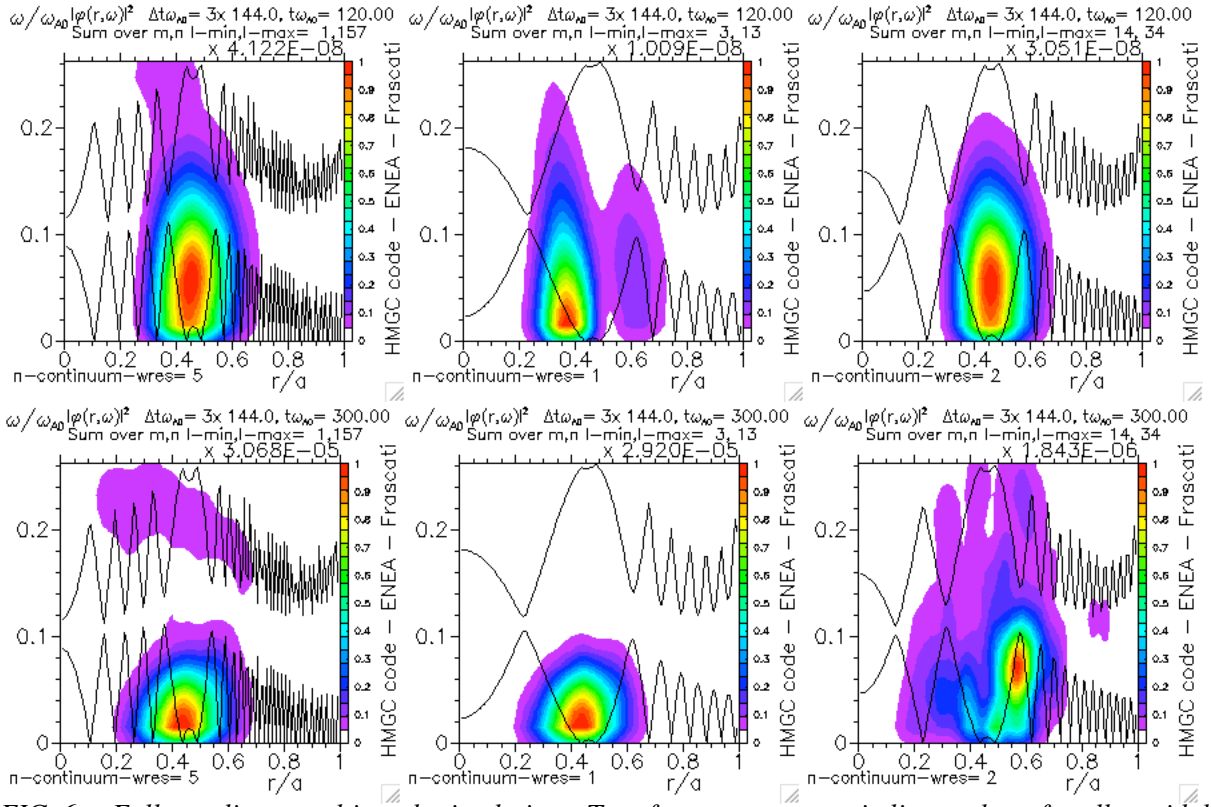

FIG. 6.: Fully nonlinear multi-mode simulation:. Top: frequency spectra in linear phase for all toroidal mode numbers (left), only $n = 1$ (centre), only $n = 2$ (right). Bottom: frequency spectra during saturated phase for all toroidal mode numbers (left), only $n = 1$ (centre), only $n = 2$ (right).

$n = 2 - 4$, in spite of its lower linear growth rate. Note, however, that such conclusion could be strongly dependent on the detailed structure of the low-frequency portion of the Alfvén continuum. Such structure could be modified both because of slight variations of the q_{min} value (cf. FIG. *3.*) as well as including additional physics in the model. In particular, the $O(\epsilon^3)$ reduced MHD equations in the zero-$\beta_{\rm bulk}$ approximation neglect sound waves and geodesic curvature couplings. If such effects were properly retained [3], a new gap in the low frequency range would form, where Beta induced Alfvén Eigenmodes (BAEs) could exist.

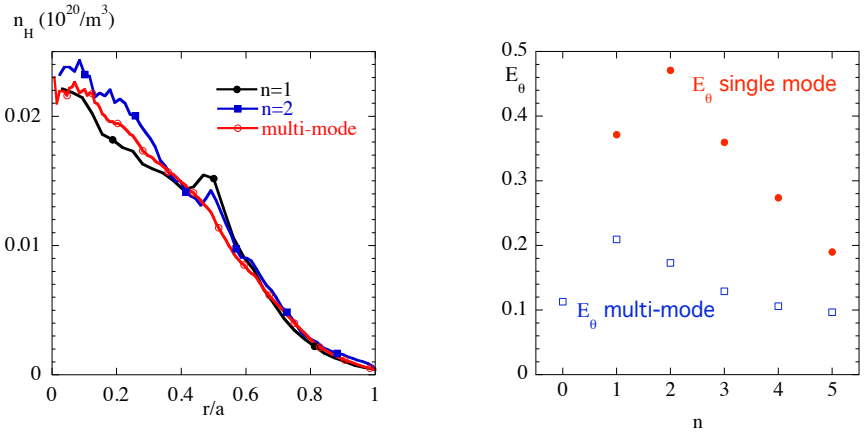

FIG. 7.: (Left): fully nonlinear multi-mode simulation compared with single-n ($n = 1$ and $n = 2$) simulations: energetic particle density profiles at saturation. (Right) saturation level of poloidal electric field of fully nonlinear simulation compared with single-n simulations.

References

[1] ZONCA, F., et al., "Transition from weak to strong energetic ion transport in burning plasmas", Nucl. Fusion **45** (2005) 477–84.

[2] ZONCA, F., et al., "Physics of burning plasmas in toroidal magnetic confinement devices", Plasma Phys. Contr. Fusion **48** (2006) B15–28.
[3] CHEN, L. and ZONCA, F., "Theory of Alfvén waves and energetic particle physics in burning plasmas", Nucl. Fusion **47** (2007) S727–34.
[4] BRIGUGLIO, S. et al., "Hybrid magnetohydrodynamic-particle simulation of linear and nonlinear evolution of Alfvén modes in tokamaks", Phys. Plasmas **5** (1998) 3287–301.
[5] TODO, Y., et al., "Nonperturbative effects of energetic ions on Alfvén eigenmodes", Proc. 20th Int. Conf. on Fusion Energy 2004 (Vilamoura, 2004) (Vienna: IAEA) CD-ROM file TH/3-1Ra and http://www-naweb.iaea.org/napc/physics/fec/fec2004/datasets/index.html.
[6] CHEN, L., "Theory of magnetohydrodynamic instabilities excited by energetic particles in tokamaks", Phys. Plasmas **1** (1994) 1519–22.
[7] BRIGUGLIO, S., et al., "Hybrid magnetohydrodynamic-gyrokinetic simulation of toroidal Alfvén modes", Phys. Plasmas **2** (1995) 3711.
[8] VLAD, G., et al., "Alfvénic instabilities driven by fusion generated alpha particles in ITER scenarios", Nucl. Fusion **46** (2006) 1–16.
[9] SHINOHARA, K., et al., "Energetic particle physics in JT-60U and JFT-2M", Plasma Phys. Contr. Fusion **46** (2004) S31–45.
[10] BRIGUGLIO, S., et al., "Particle simulation of bursting Alfvén modes in JT-60U", Phys. Plasmas **14** (2007) 055904.
[11] STRAUSS, H.R., "Dynamics of high beta tokamaks", Phys. Fluids **20** (1977) 1354.
[12] IZZO, R., et al., "Effects of toroidicity on resistive tearing modes ", Phys. Fluids **26** (1983) 2240.
[13] FRIEMAN, E.A. and CHEN, L., "Nonlinear gyrokinetic equations for low-frequency electromagnetic waves in general plasma equilibria", Phys. Fluids **25** (1982) 502.
[14] LEE, W.W., "Gyrokinetic particle simulation model", Journal of Comp. Physics **72** (1987) 243.
[15] PARK, W., et al., "Three-dimensional hybrid gyrokinetic-magnetohydrodynamics simulation", Phys. Fluids **B 4** (1992) 2033.
[16] HEIDBRINK, W.W., et al., "Central flattening of the fast-ion profile in reversed-shear DIII-D discharges", Nucl. Fusion **48** (2008) 084001.
[17] BUDNY, R.V. et al., "Simulations of alpha parameters in a TFTR DT supershot with high fusion power", Nucl. Fusion **35** (1995) 1497.
[18] LAO, L.L. et al., "Reconstruction of current profile parameters and plasma shapes in tokamaks", Nucl. Fusion **25** (1985) 1611.
[19] TAKECHI, M., et al., "Property of Alfvén eigenmode in JT-60U reversed shear and weak shear discharges", Proc. 19th Int. Conf. on Fusion Energy 2002 (Lyon, 2002) (Vienna: IAEA) CD-ROM file EX/W-6 and http://www.iaea.org/programmes/ripc/physics/fec2002/html/fec2002.htm.
[20] SHARAPOV, S.E., et al., "MHD spectroscopy through detecting toroidal Alfvén eigenmodes and Alfvén wave cascades", Phys. Lett. A **289** (2001) 127.
[21] VAN ZEELAND, M.A., et al., "Radial Structure of Alfvén Eigenmodes in the DIII-D Tokamak through Electron-Cyclotron-Emission Measurements", Phys. Rev. Lett. **97** (2006) 135001 97, 135001 (2006).
[22] VAN ZEELAND, M.A., et al., "Reversed shear Alfvén eigenmode stabilization by localized electron cyclotron heating", Plasma Phys. Contr. Fusion **50** (2008) 035009.